Monatshefte für Chemie - Chemical Monthly (2020) 151:1511–1523
https://doi.org/10.1007/s00706-020-02683-6

ORIGINAL PAPER

# Electrochemical monitoring of metal ions removal in $Fe^0/H_2O$ systems: competitive effects of cations $Zn^{2+}$, $Pb^{2+}$, and $Cd^{2+}$

**Marquise Touomo-Wouafo[1,3] · Joël Donkeng-Dazie[2,3] · Ivan Jirka[3] · Brice D. Btatkeu-K[1] · Jean Bosco Tchatchueng[1] · Chicgoua Noubactep[4] · Jiří Ludvík[3]**

Received: 27 June 2020 / Accepted: 1 September 2020 / Published online: 7 October 2020


## Abstract

Metallic iron ($Fe^0$) is a reactive material that is widely used for industrial water treatment. The course of the metal ion removal process using $Fe^0$ (iron powder) was monitored electrochemically (differential pulse polarography). As probe species, $Zn^{2+}$, $Pb^{2+}$, and $Cd^{2+}$ were selected for their different (1) adsorptive affinity to iron corrosion products (FeCPs), (2) redox properties, (3) precipitation ability at various pH. Batch experiments were carried out with binary ($Zn^{2+}$/ $Pb^{2+}$ and $Zn^{2+}$/ $Cd^{2+}$) and ternary ($Zn^{2+}$/$Cd^{2+}$/$Pb^{2+}$) systems to reveal the mutual interference of these cations. Detailed time monitoring of iron aging for up to 14 days as well as concentration decay of individual removed cations represent important data for mechanistic discussions. The aqueous concentration of $Fe^{2+}$ was also monitored. FeCPs were characterized using X-ray photoelectron spectroscopy (XPS) and scanning electron microscopy (SEM). Results showed that the presence of $Pb^{2+}$ delays the $Zn^{2+}$ removal whereas the presence of $Cd^{2+}$ in solution accelerates its removal. The removal of $Pb^{2+}$ by FeCPs was not affected by the presence of $Zn^{2+}$ and $Cd^{2+}$, moreover, the $Pb^{2+}$ inhibited the effect of $Cd^{2+}$ on the removal of $Zn^{2+}$. XPS has proven existence of $Fe_2O_3$ and hydrated Fe oxidic phase, whilst the SEM showed that the original Fe grains were partly dissolved into buffered ambient under formation of fine particles of FeCPs. Results confirm that reductive transformation of any contaminant in a $Fe^0/H_2O$ system is the consequence and not the cause of iron corrosion.

### Graphic abstract

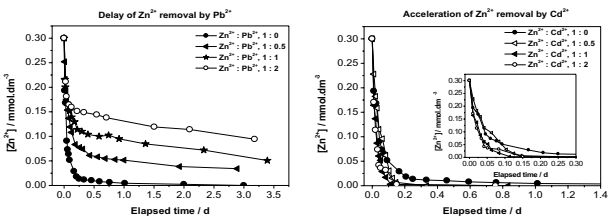


**Keywords** Heavy metals · Multiple cations · Electrochemistry · Water treatment · Aged zero-valent iron

✉ Jiří Ludvík
jiri.ludvik@jh-inst.cas.cz

1 National School of Agro-Industrial Sciences, University of Ngaoundere, P.O. Box 455, Ngaoundere, Cameroon

2 Chemical Engineering and Mineral Industries School, University of Ngaoundere, P.O. Box 454, Ngaoundere, Cameroon

3 J. Heyrovsky Institute of Physical Chemistry, Academy of Sciences of the Czech Republic, 182 23 Prague 8, Czech Republic

4 Angewandte Geologie, Universität Göttingen, Goldschmidtstraße 3, 37077 Göttingen, Germany

## Introduction

The presence of heavy metals in wastewater generated from industrial activities such as mining and smelting and battery manufacturing [1] is one of the most serious environmental problems worldwide. Heavy metals persist in the environment and pose a high risk to ecosystems and human health [2]. There is a crucial need for low-cost, effective approached to remove heavy metals from wastewater. Metallic iron materials—$Fe^0$ (or zero-valent iron—ZVI) has been

**Table 1** Diversity of experimental conditions (appeared in literature) for batch experiments using metallic iron and various types of FeCPs for $Zn^{2+}$, $Cd^{2+}$, and $Pb^{2+}$ removal

| Type | Quantity/g | pH | $[Zn^{2+}]$/ mmol/dm$^3$ | $[Cd^{2+}]$/ mmol/dm$^3$ | $[Pb^{2+}]$mmol/ dm$^3$ | Duration/h | Temp/°C | Volume/ cm$^3$ | Mixing | References |
|---|---|---|---|---|---|---|---|---|---|---|
| ZVI | 40–1000 | 3–13 | 50[b] | – | – | 24 | n.s | 1000 | Shaker | [14] |
| Hematite | 5–8 | 2.40–7.10 | – | (100–1000)[a] | (100–1000)[a] | 0.25–2 | RT | 100 | Shaker | [31] |
| nZVI | 2 | 4.0 ± 0.2 | 0–0.5 | 0–0.412 | 0–0.29 | 48 | 21 ± 2 | 100 | Rot. shaker | [40] |
| nZVI | 0,03 | 4–10 | 1 | 1 | – | 0–72 | RT | 60 | Agitation | [39] |
| Goethite | (0.1 and 1)[b] | 4–8 | – | $4.45\times10^{-3}$ | $4.69\times10^{-3}$ | 2 and 4 | n.s | n.s | Bath shaker | [32] |
| Ferrihydrite | ($10^{-3}$)[c] | 3–10 | $5\times10^{-3}$ and $1\times10^{-2}$ | $10^{-2}$ | $10^{-2}$ | 1–3 | n.s | 10–40 | Rotation | [47] |
| $Fe_2O_3$•$H_2O$ | ($10^{-3}$)[c] | 4.5–8 | $5\times10^{-2}$ | $5\times10^{-4}$ to $5\times10^{-2}$ | $5\times10^{-2}$ | 4 | 20 and 25 | n.s | n.s | [48] |
| Fe gel | (0.093)[c] | 4–10 | 0.125 | 0.125 | 0.125 | 3 | n.s | 25 | n.s | [49] |
| goethite | 0.02 | 4.7–8 | 2.62 | 2.62 | 2.62 | 25 | 20 | 40 | n.s | [33] |
| Hydrous iron oxides | ($6.25\times10^{-3}$ and $5\times10^{-2}$)[c] | 4–8 | 1 | 1 | 0.5–4 | 0.166 | RT | 100 | n.s | [34] |

*n.s.* not specified, *RT* room temperature, *nZVI* nano zero-valent iron

[a]Concentration expressed in ppm

[b]Quantity expressed in g/dm$^3$

[c]Quantity expressed in mmol/dm$^3$

used for this purpose for quite a long time [3–5] however, on a pure pragmatic approach [6].

Metallic iron materials ($Fe^0$) have been broadly utilized in the water remediation industry for the past three decades [5, 7–14]. The interactions of $Fe^0$ with water ($Fe^0/H_2O$ systems) involves the in-situ generation of solid iron corrosion products (FeCPs), which in turn act as contaminant scavengers [6, 15–20]. The efficiency of freshly generated in-situ FeCPs for the removal of dyes [18, 21], fluoride ion [20, 22], and $Zn^{2+}$ [19] has been investigated in batch systems. In addition, Touomo-Wouafo et al. [19] monitored the time-dependent changes in a $Fe^0/Zn^{2+}/H_2O$ system to better characterize the remediation process. The main outcome of these studies is that $Fe^0$ is not the agent reducing directly the cations of contaminants under environmental conditions.

This conclusion is present in the literature since 2007 [23, 24] but has been largely ignored by active researchers [6, 25, 26]. A recent overview article by Hu et al. [27], summarizes the complexity of the $Fe^0/H_2O$ system and recalls that contaminant removal is an inherent property of aqueous iron corrosion. This implies that upon proper design each polluted water can be treated using $Fe^0$. For this reason, to gain more information about the efficiency of each system, either several $Fe^0$ materials are used for a single-contaminant or multi-contaminant systems are used for the same material, The approach used herein is the latter. Really polluted wastewaters contain more than one heavy metal. Therefore investigation of the effectiveness of FeCPs for the removal of multiple competing cations is very important [28–30].

In scientific literature considering $Fe^0$ as a stand-alone reducing agent, the diversity of used experimental conditions renders the comparison of achieved results almost impossible (Table 1). It is evident from the Table 1 that the majority of selected studies deals with defined oxides like hematite [31], goethite [32, 33], or hydrous iron oxides [34]. Those systems are limited by the fact that there is not a continuous production of in-situ FeCPs, the time development is not followed and, therefore, the interpretation of metals removal is limited to adsorption at equilibrium. On the other hand, using $Fe^0$, the removal of contaminants is governed by a synergy of freshly and continuously in situ-generated FeCPs leading to adsorption and precipitation/co-precipitation. In this case, however, detailed time dependence is necessary to understand more deeply the remediation mechanisms.

Recently, Vollprecht et al. [14] investigated the removal of multiple metal cations from wastewater using $Fe^0$. In their batch experiments, substantial differences in reactivity towards FeCPs were observed. These differences influencing effectivity of metals removal are caused among others by different conditions (e.g. pH) and also by the presence of both anions and cations in the tested water. However, in their paper, there is not specified the $Fe^0$

material (size, surface), its aging is not considered and some important metal cations are missing.

For the present work, fresh iron powder -200 mesh (74 µm) with defined size and surface [19] was used as the remediation agent and $Zn^{2+}$, $Cd^{2+}$ and $Pb^{2+}$ ions have been chosen as contaminants because they are commonly present in wastewater and because they have different (1) adsorptive affinity to FeCPs, (2) redox properties, (3) precipitation ability at various pH. The study is performed with binary ($Zn^{2+}/Pb^{2+}$ and $Zn^{2+}/Cd^{2+}$) and ternary ($Zn^{2+}/Cd^{2+}/Pb^{2+}$) mixtures of various proportions of ions, in batch systems at pH 5.5 which is the optimum pH for the removal of $Zn^{2+}$ obtained from our previous study [19]. The concentration changes of aqueous $Fe^{2+}$, $Zn^{2+}$, $Cd^{2+}$, and $Pb^{2+}$ are monitored within the time span from minutes to 14 days, using differential pulse polarography (DPP). The DPP technique was chosen because it was possible to follow simultaneously the current (concentration) of several metal ions in aqueous solution. The X-ray photoelectron spectroscopy (XPS) and scanning electron microscopy (SEM) are used for the characterization of FeCPS after the remediation process with the aim to intercept and describe the form of removed metals.

The purpose of the present study is to investigate (1) the efficiency of differently aged FeCPs for the removal of multiple competing heavy metals; (2) the time development of all processes; (3) the iron powder after the process with adsorbed/precipitated/reduced products; (4) the mutual influence of the present metal cations being simultaneously in the mixture because their interference is very probable due to their different adsorptive affinity to FeCPs, and different redox properties. All experiments should contribute to the explanation of all observed effects (for example the reason and relevance of the "induction period" at the beginning of the ZVI aging) and thus to detailed understanding of the mechanism of removal of selected heavy metals.

## Results and discussion

### Monitoring of $Fe^0$ pre-corrosion

When 0.8 g of $Fe^0$ was added in 0.1 mol/dm$^3$ acetate buffer solution pH 5.5, in the presence of air oxygen (in the absence of $Zn^{2+}$, $Cd^{2+}$, and $Pb^{2+}$), typically only $Fe^{2+}$ was identified at − 1.4 V vs. SCE and its concentration–time profile is depicted in Fig. 1.

It can be observed at the Fig. 1a that the concentration of $Fe^{2+}$ gradually increases then reaches a maximum after approx. 3 h, then remains unchanged during few hours (where a plateau is formed). Thereafter, $Fe^{2+}$ starts to decreases progressively with time. An increase of pH up to 6.7 was noticed during the first 3 h (although the experiment is performed in buffered solution, initial pH 5.5), afterwards the pH diminishes progressively and returns back to its initial value. Similar observation has been reported by Touomo-Wouafo et al. [19]. The authors explained this effect by the corrosion of iron by water with dissolved oxygen leading to the release of $Fe^{2+}$ and $OH^-$ in solution which will progressively transformed to FeCPs [19].

The detailed view of this experiment reveals an "induction period" of the corrosion which occurs during the first 30 min of experiment (Fig. 1b) which could be attributed to the activated time of iron. In that period $Fe^{2+}$ is not released and its concentration in solution is zero. The same kind of "induction period" was reported in our previous study [19]. In that study, only 0.1 g of $Fe^0$ was used, the "induction period" lasts the first 1–2 h, the pH increased up to 6.0 and then returned back to 5.5. The present investigation points out that, the "induction period" depends on the amount of $Fe^0$ used: higher amount of $Fe^0$ employed in the experiment of the same volume causes shorter "induction period" and higher pH during the maximal concentration of $Fe^{2+}$. Most probably, these effects are connected with the reaction of $Fe^0$ with dissolved oxygen in the first part of the corrosion process. The detailed interpretation of these induction periods

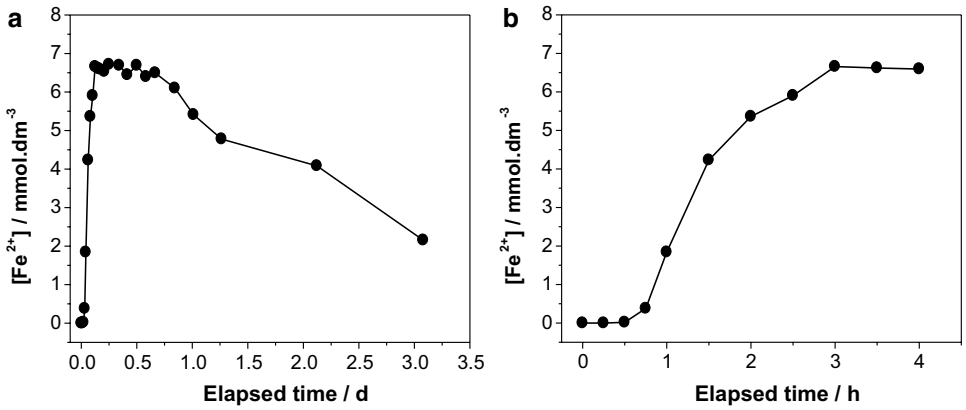


**Fig. 1** Time-dependence of the concentration of $Fe^{2+}$ ion during pre-corrosion of 0.8 g of $Fe^0$ in 199 cm$^3$ of 0.1 mol/dm$^3$ acetate buffer pH 5.5, in the presence of air oxygen. **a** From 0 to 3 days; **b** detail of the first 4 h

is the subject of our further studies. In the past, analogous kind of induction period but under different conditions was observed (without explanation) by Lavine et al. [35], who "pre-treated" $Fe^0$ by washing it with a variety of aqueous solutions, including HCl.

The preliminary experiments reveal that 0.8 g of $Fe^0$ aged 3 h was suitable, therefore, for all investigations in this study, 0.8 g of $Fe^0$ aged 3 h (time corresponding to maximum of $Fe^{2+}$ in solution) in 0.1 mol/dm$^3$ acetate buffer solution pH 5.5 was used.

## Effect of competitive cations on the removal of $Zn^{2+}$

### Binary systems

For this study, each solution contained only two target metallic cations (besides in-situ $Fe^{2+}$). The concentration of $Zn^{2+}$ is set to 0.3 mmol/dm$^3$ whilst the concentration of the competitive cation corresponds to 0.15 mmol/dm$^3$, 0.3 mmol/dm$^3$, and 0.6 mmol/dm$^3$ respectively for the ratio $Zn^{2+}$:$M^{2+}$ (M represents Pb or Cd), 1:0.5, 1:1, and 1:2.

#### *Effect of $Pb^{2+}$ on the removal of $Zn^{2+}$*

The time-dependence of $Zn^{2+}$ decay after addition of 1 cm$^3$ of binary metal mixed stock solutions ($Zn^{2+}$/$Pb^{2+}$ of various ratio) in 199 cm$^3$ of acetate buffer containing 0.8 g of $Fe^0$ prior aged 3 h is presented in Fig. 2.

From Fig. 2a, it is evident that in the absence of $Pb^{2+}$ (ratio $Zn^{2+}$:$Pb^{2+}$, 1:0), the majority of $Zn^{2+}$ ion is removed within the first hours and completely after 3 days, whereas in the increasing presence of $Pb^{2+}$ the remediation occurs slower and slower and, finally, 97% of $Zn^{2+}$ is removed after 14 days. When the experiment is evaluated at short reaction time (Fig. 2b), it is obvious that the efficiency of $Zn^{2+}$ removal using aged $Fe^0$ decreases by increasing concentration of $Pb^{2+}$ ion in solution. Accordingly, only 88.6, 83, and 68.6% of $Zn^{2+}$ removal is obtained respectively with 0.15, 0.3, and 0.6 mmol/dm$^3$ of $Pb^{2+}$ concentration in solution after 3 days. Based on these results, it can be concluded that, the $Pb^{2+}$ ion delays substantially removal of $Zn^{2+}$ from the solution and the final percentage of remaining $Zn^{2+}$ is higher.

Besides the above results, monitoring of the $Pb^{2+}$ concentration shows that $Pb^{2+}$ ions completely disappear shortly after their addition to the solution. Hence, interaction of $Pb^{2+}$ with the aged iron (or with the present solution) is fast regardless to the ratio $Zn^{2+}$:$Pb^{2+}$. The same result was obtained in the absence of $Zn^{2+}$ in solution. Thus, $Zn^{2+}$ ion does not influence the removal of $Pb^{2+}$ using ZVI aged 3 h. Similar finding has been reported by Gadde and Laitinen [34], in the binary system $Pb^{2+}$/$Zn^{2+}$ using hydrous iron and manganese oxides. The authors mentioned that lead is adsorbed more strongly than any other metal ion studied. However, the role of pH should be also taken into account in the evaluation and interpretation of the data from the Fig. 2a, b. Since the pH of the solution reaches 6.7 after 3 h of aging of iron in the absence of heavy metals, the precipitation of their hydroxides could likewise contribute to the observed rapid removal of $Pb^{2+}$. This result is consistent with those of Khorshidi and Azadmehr [31]. Using hematite as adsorbent, the authors underlined that at pH more than 6, lead is entirely precipitated into $Pb(OH)_2$. However, those authors did not prove the presence of $Pb(OH)_2$.

All these observations highlight the ion-selective nature of FeCPs including the present solution) towards the present target heavy metals. As a result, after several hours the aged FeCPs mixture reacts preferentially with $Pb^{2+}$ (or with its precipitate) than with $Zn^{2+}$. It may cause blocking of the reactive sites at the surface of the aged iron powder and the removal of the remaining $Zn^{2+}$ occurs substantially slower. This outcome is consistent with Pauling electronegativity values of each investigated cation which are 2.33 and 1.65, respectively, for $Pb^{2+}$ and $Zn^{2+}$ [36], hence higher electronegativity causes stronger interaction with FeCPs. The obtained result also matches with the hardness index of target cations, 0.131 and 0.115 for $Pb^{2+}$ and $Zn^{2+}$, respectively, and the values of logarithm of the first hydrolysis constant

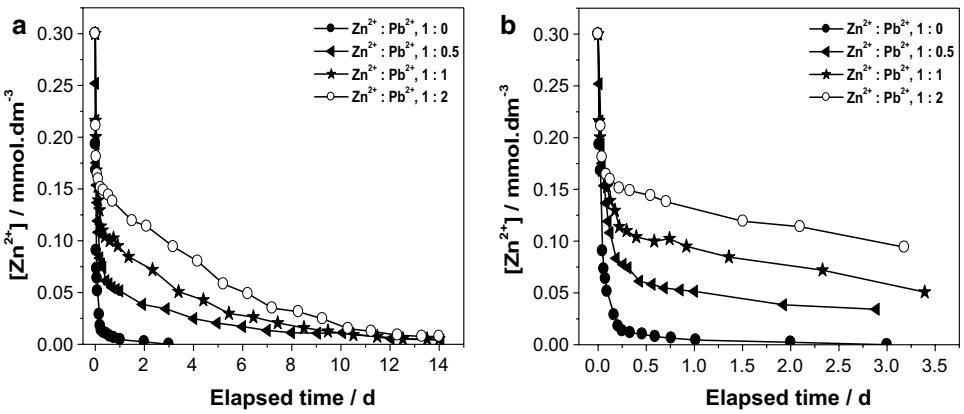


**Fig. 2** Time-dependence of the decrease of the $Zn^{2+}$ ion concentration during remediation using $Fe^0$ (0.8 g of $Fe^0$ prior aged 3 h in 200 cm$^3$ of 0.1 mol/dm$^3$ buffer pH 5.5, in the presence of air oxygen) of various ratio $Zn^{2+}$:$Pb^{2+}$. **a** From 0 to 14 days; **b** detail view from 0 to 3.5 days

of cations which are −7.6 and −9, respectively, for $Pb^{2+}$ and $Zn^{2+}$ [36].

In addition of these results, it was also observed a progressive vanishing of $Fe^{2+}$ concentration in solution with time. This decrease underlines a continuous production of FeCPs and the formation of an oxide layer on $Fe^0$ ("passivation") [37, 38]. This outcome was expected since the consumption of $Fe^{2+}$ by dissolved oxygen in water or $OH^-$ leads to $Fe^{3+}$ and $Fe(OH)_2$. $Fe^{3+}$ thereafter reacts with $OH^-$ in solution to form $Fe(OH)_3$. Both $Fe(OH)_2$ and $Fe(OH)_3$ are later transformed to FeOOH, $Fe_2O_3$ and $Fe_3O_4$ [19].

### *Effect of $Cd^{2+}$ on the removal of $Zn^{2+}$*

In contrast to the results of above section, the presence of $Cd^{2+}$ promotes the removal of $Zn^{2+}$ in solution. As a result, in the binary $Zn^{2+}/Cd^{2+}$ system the remediation of $Zn^{2+}$ by aged $Fe^0$ is almost completed after 0.2 days which corresponds to approx. 4 h while in the absence of $Cd^{2+}$ such result is achieved after 3 days (Fig. 3c). The facilitation of $Zn^{2+}$ removal by $Cd^{2+}$ requires detailed studies and will be the subject of our further study.

The time-dependence of the decrease of the $Cd^{2+}$ ion concentration (in the absence or in the presence of $Zn^{2+}$) depicted in Fig. 3b displays a slight decrease of $Cd^{2+}$ ion concentration during the first day then reaches a pseudo-equilibrium in solution. After 6 days, a new decrease of $Cd^{2+}$ ion concentration is observed. This behavior might be due to the fact that, the FeCPs formed at the equilibrium (after 3 h of aging) are not suitable for the removal of $Cd^{2+}$ but appropriate for $Zn^{2+}$ removal (Fig. 3c). On the other hand, after 6 days, the FeCPs are convenient for the trapping of $Cd^{2+}$.

It is also evident from the Fig. 3c that the order of effectiveness of metal ions removal by aged $Fe^0$ is as follows: $Zn^{2+} > Cd^{2+}$. Like in the previous case, this is consistent with the hardness index of cations, 0.115 and 0.081 for $Zn^{2+}$ and $Cd^{2+}$, respectively, and the values of logarithm of the first hydrolysis constant of cations which are -9 and -10.1, respectively, for $Zn^{2+}$ and $Cd^{2+}$ [36].

When considering the inverse case (how $Zn^{2+}$ ions affect the removal of $Cd^{2+}$), the percentage of removal of $Cd^{2+}$ obtained after 14 days of reaction is moderately dependent on the $Zn^{2+}$:$Cd^{2+}$ ratio in a remarkable manner: Subsequently, 65, 67, 63, and 75% of $Cd^{2+}$ are removed respectively in the ratio $Zn^{2+}$:$Cd^{2+}$, 0:1, 1:0.5, 1:1, 1:2. It is noticed that the $Zn^{2+}$ slightly diminishes the percentage of the $Cd^{2+}$removal. Analogous result has been reported by Boparai et al. [39]. In their work, the authors attributed this effect to the chemical similarities between $Cd^{2+}$ and $Zn^{2+}$, consequently they may strongly compete for the

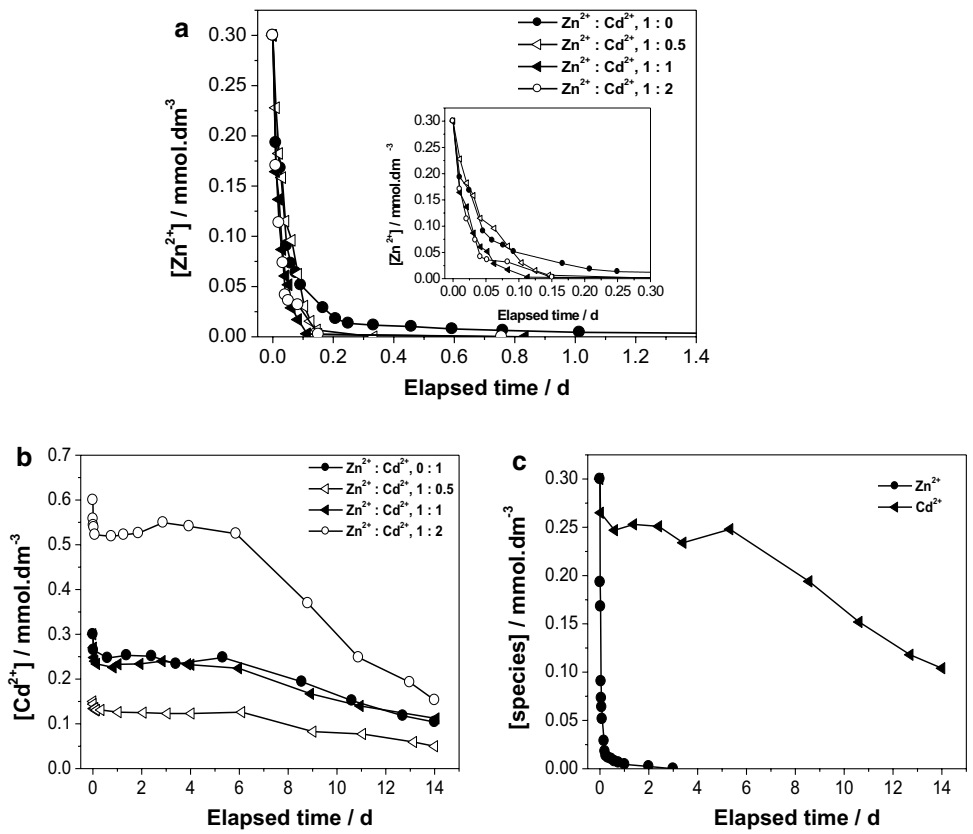


**Fig. 3** Time-dependence of the decrease of the **a** $Zn^{2+}$, **b** $Cd^{2+}$ ions during remediation using ZVI at various $Zn^{2+}$:$Cd^{2+}$ ratio. (0.8 g of $Fe^0$ prior aged 3 h in 199 $cm^3$ of 0.1 $mol/dm^3$ acetate buffer pH 5.5, in the presence of air oxygen). **c** Comparison of the time-dependence of the concentration decay of $Zn^{2+}$ and $Cd^{2+}$, both 0.3 $mmol/dm^3$ at the same conditions

same adsorption sites. However, in their study, they have not considered the effect of $Cd^{2+}$ on the removal of $Zn^{2+}$.

### Ternary systems

In the present study, various ratios $Zn^{2+}$:$Cd^{2+}$:$Pb^{2+}$ were investigated namely: 1:0.5:0.5, 1:0.5:1, 1:1:0.5, 1:1:1, 1:1:2, 1:2:1, 1:2:2, where the concentration of $Zn^{2+}$ was constant and set to 0.3 mmol/dm$^3$ whilst the concentration of competitive cations varied from 0.15 to 0.6 mmol/dm$^3$.

The Fig. 4 shows the concentration evolution of $Zn^{2+}$ with time during its remediation using $Fe^0$ (aged 3 h in 199 cm$^3$ of 0.1 mol/dm$^3$ acetate buffer pH 5.5) at various ratio $Zn^{2+}$:$Cd^{2+}$:$Pb^{2+}$ (for clarity all eight dependences were divided into two graphs). Although the systems were analyzed in detail for 14 days, the presented dependences are described for the contact time 3.5 days when the data are the most informative.

Generally, it appeared that the percentage of removal of $Zn^{2+}$ after 14 days is more than 98% from all data of Fig. 4, except in the ratio 1:0:0, where $Zn^{2+}$ is completely removed after 3 days, hence it is evident that the presence of both competitive cations delays the removal of $Zn^{2+}$ in solution. This is mainly owing to the already mentioned slowing effect of $Pb^{2+}$ upon the removal of $Zn^{2+}$, which inhibited the slightly accelerating effect of $Cd^{2+}$.

It was also observed a rapid disappearing of $Pb^{2+}$ at the initial stage of reaction as it was the case in the binary system $Zn^{2+}$/$Pb^{2+}$. Accordingly, the presence of $Cd^{2+}$ does not have any influence on the removal of $Pb^{2+}$. Moreover, pseudo-equilibrium in the removal of $Cd^{2+}$ appeared likewise in the ternary system with a short duration in comparison of binary system.

The percentage of removal of $Zn^{2+}$ ions after approx. 3 days reaction time (taken from the data of Fig. 4) and those of $Cd^{2+}$ ions at 14 days reaction time are presented in the Table 2. It follows from the data of Table 2 that after 3 days more than 90% removal of $Zn^{2+}$ is obtained when concentration of $Cd^{2+} \geq Pb^{2+}$. These results confirmed our earlier observation obtained in the binary systems where it was highlighted that the $Cd^{2+}$ accelerates whilst the $Pb^{2+}$ reduces the $Zn^{2+}$ removal percentage (cf. Fig. 2b). It is also evident that for the equal concentration of $Cd^{2+}$ and $Pb^{2+}$, a "neutralization" of rather opposing effects of $Cd^{2+}$ and $Pb^{2+}$ on the $Zn^{2+}$removal occurs.

**Table 2** Percentage of $Zn^{2+}$ (after 3 days) and $Cd^{2+}$ (14 days) removal from the ternary mixtures using $Fe^0$ aged for 3 h

| $Zn^{2+}$:$Cd^{2+}$:$Pb^{2+}$ ratio | Removal of $Zn^{2+}$/% | Removal of $Cd^{2+}$/% |
|---|---|---|
| 1:0.5:0.5 | 91 | 55 |
| 1:0.5:1 | 87 | 52 |
| 1:1:0.5 | 96 | 59 |
| 1:1:1 | 96 | 58 |
| 1:1:2 | 84 | 58 |
| 1:2:1 | 99 | 65 |
| 1:2:2 | 91 | 64 |

A close comparison of percentages of removal of $Cd^{2+}$ obtained in $Zn^{2+}$/$Cd^{2+}$ system with those presented in Table 2 reveals that any addition of $Pb^{2+}$ in solution decreases the percentage of removal of $Cd^{2+}$ which is in agreement with the early observation of Gadde and Laitinen [34].

According to the above-mentioned results, the following order of decreasing efficiency of metal cations removal by aged $Fe^0$ can be deduced: $Pb^{2+} > Zn^{2+} > Cd^{2+}$. This is analogous to the decrease order of selectivity of FeCPs towards the investigated metallic cations reported by several authors [32–34, 40], using goethite, iron nanoparticles, hydrous iron, and manganese oxides.

Though no explanation of such order was given by some of those authors, the obtained order correlates well with the hardness index of investigated cations which are respectively for $Pb^{2+}$, $Zn^{2+}$, and $Cd^{2+}$ 0.131, 0.115, and 0.081 as reported Kinraide and Yermiyahu [36] and also with the values of logarithm of first hydrolysis constant of each cations, −7.6, −9, and −10.1, respectively, for $Pb^{2+}$, $Zn^{2+}$, and $Cd^{2+}$ [36]. In any case, one has to keep in mind that it is hardly possible

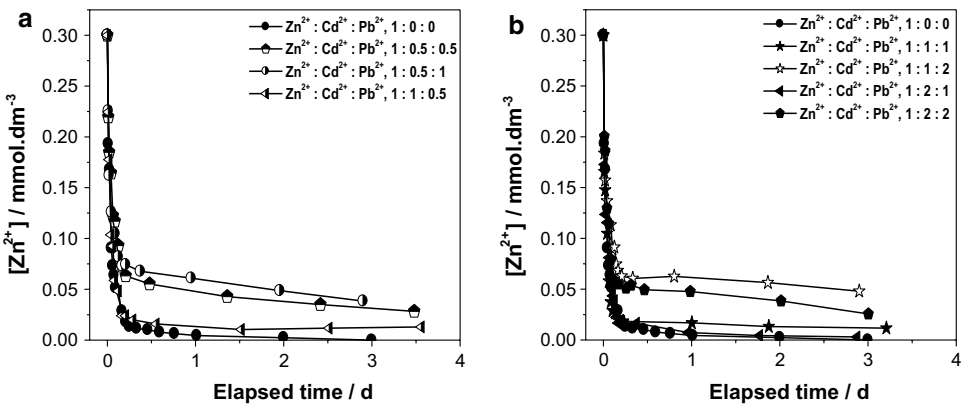


**Fig. 4** Time-dependence of the decrease of the $Zn^{2+}$ ion concentration during remediation using $Fe^0$ (0.8 g of $Fe^0$ prior aged 3 h in 199 cm$^3$ of 0.1 mol/dm$^3$ acetate buffer pH 5.5, in the presence of air oxygen) of various ratio $Zn^{2+}$:$Cd^{2+}$:$Pb^{2+}$ from 0 to 3.5 days (for clarity the set of eight dependences was divided into two graphs)

to find one single well-fitting correlation because the remediation mechanism of these three cations is based on different processes: acidobasic at higher pH, (co-)precipitation, adsorption on FeCPs and/or redox. The elucidation of more detailed mechanism distinguishing role of various conditions is in our next plans.

## Characterization of the solids by SEM and XPS—mechanistic considerations

The surface of the iron powder exposed to buffered water ambient before and after addition of $Zn^{2+}$, $Cd^{2+}$, and $Pb^{2+}$ ions was characterized by X-ray photoelectron spectroscopy (XPS) and its morphology by scanning electron microscopy (SEM).

The aging of $Fe^0$ powder in the buffer is naturally accompanied by extensive corrosion of $Fe^0$ powder which changes substantially the surface morphology. As follows from SEM results (Fig. 5) the originally smooth grains of the sample **1** (bare Fe powder taken directly from the original flask) after 10 days in the buffer (sample **3**), they are partly dissolved and simultaneously/consequently covered by a thick layer of FeCPs fine crystals with high specific surface. Aging is, therefore, a multistep process which manifests itself by the observed "induction period" (cf. Fig. 1b) and by unusual shape of the $Fe^{2+}$ time dependence (cf. Fig. 1a), and causes curious beginning of all ions removal (cf. Figs. 2, 3).

The survey photoelectron spectra of the samples **4** (top) and **7** (bottom) sputtered by $Ar^+$ ions ($t = 5$ min) measured at low resolution are depicted in Fig. 6. The spectra are normalized relative to the unit height of O 1 s line for comparison. The low energy regions of spectra (< 520 eV, in red) are expanded to make more visible low intensive photoelectron lines. The survey spectra of the samples **1**, **2**, **3**, and **6** are qualitatively the same as the spectrum of the sample **4**, spectrum of the sample **5** qualitatively corresponds to that of the sample **7**. The same results were obtained from the spectra of the non-sputtered samples.

The assigned photoelectron and Auger lines detected in investigated samples and presented in the Table 3 show that

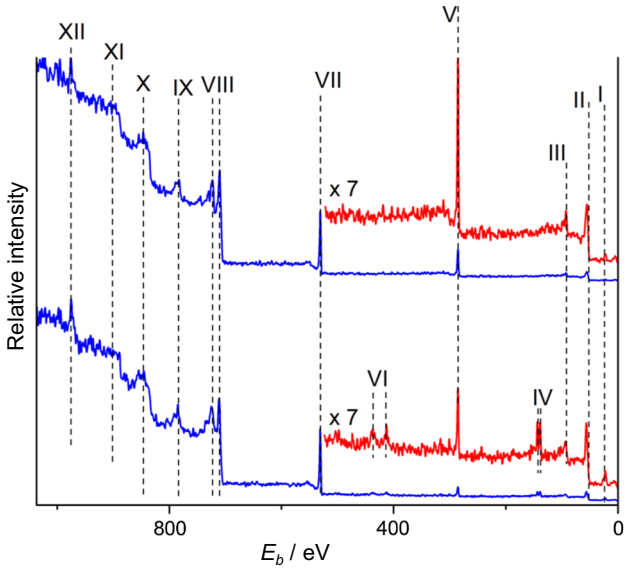


**Fig. 6** Photoelectron survey spectra of the samples **4** (top) and **7** (bottom) sputtered by $Ar^+$ ions ($t = 5$ min) measured at low resolution

all samples are composed from Fe, C, and O. Presence of Pb was detected in the samples **5** and **7**. On the other hand, the presence of Si in the sample **1**, Cd in the sample **6**, and Zn in the samples **4** and **7** was not observed on this survey spectrum because their concentration was close to the detection limit. Confirmation of these elements was done using measurements at high resolution (Fig. 7) (Si found in the sample **1** can be due to the presence of trace of Si in the original container of $Fe^0$ powder). Results of quantitative XPS analysis of the samples **1**–**7** are summarized in Table 4. Concentrations of Fe, C, O, Cd, Pb, and Zn are expressed in atomic %, calculated using Eq. (1). Intensities of photoelectron spectra were calibrated using Wagner sensitivity factors [41].

To discuss the effect of exposition of the sample to buffered water ambient the photoelectron Fe $2p_{3/2}$, C 1s, and O 1s spectra of the samples **1** and **3** measured in high

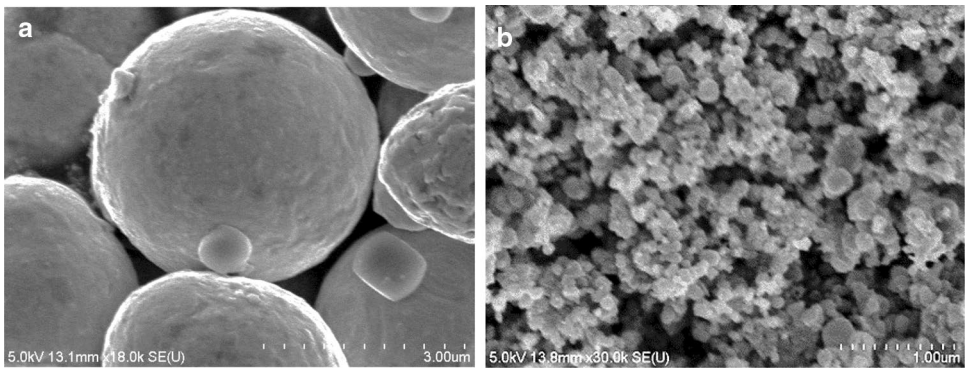


**Fig. 5** SEM images of the sample **1** (**a**) and **3** (**b**)

**Table 3** Assignment of the photoelectron and Auger spectra measured at low resolution

| Line # | $E_b$ /eV | assignment |
|---|---|---|
| I | 23 | O 2s |
| II | 56 | Fe $3p_{3/2,1/2}$ |
| III | 93 | Fe 3s |
| IV | 137, 146 | Pb $4f_{7/2,5/2}$ |
| V | 285 | C 1s |
| VI | 414, 446 | Pb $4d_{5/2,3/2}$ |
| VII | 531 | O 1s |
| VIII | 713, 727 | Fe $2p_{3/2,\ 1/2}$ |
| IX | 783 | Fe K $L_{2,3}L_{2,3}$[a] |
| X | 847 | Fe K $L_1L_{2,3}$[a] |
| XI | 900 | Fe K $L_1L_1$[a] |
| XII | 976 | O K $L_{2,3}L_{2,3}$[a] |

[a]Auger spectra

resolution before (blue color) and after $Ar^+$ sputtering for **7** min (red color) are compared in Fig. 8.

The Fe $2p_{3/2}$ spectra (line I) at binding energy $E_b \sim 711.4$ eV measured before sputtering correspond to the oxide layer ($Fe_2O_3$) on the surfaces of samples **1** and **3**, which can be in the case of the sample **1** almost completely eliminated by sputtering by $Ar^+$ ions for 7 min. Asymetric line (II) at $E_b = 707.3$ eV observed in the sputtered sample **1** belongs to metallic Fe, its asymmetry is affected by presence of very small amounts of residual Fe oxide (cf. intensity of O 1 s line after sputtering).

Much weaker line II is present in the Fe $3p_{3/2}$ spectrum of sputtered sample **3** (cf. low energy shoulder in the spectrum) and line I is shifted to lower $E_b$. These effects reflect much thicker oxide layer of the sample **3** due to long aging of the sample **3** in the buffer. While the oxide layer can be almost quantitatively eliminated from the sample **1**, rather thick oxidic layer remained on the sample **3** even after 7 min of sputtering. Obtained findings are in line with observed intensity changes of O 1 s photoelectron spectra (Fig. 8a) and results of quantitative analysis (cf. Table 4). Sputtering further reduced surface hydrocarbon contamination of the samples.

Summary of the photoelectron Fe $2p_{3/2,1/2}$, O 1 s, and C 1 s spectra of the samples **3**—**7** measured at high resolution is depicted in Fig. 8b. To minimize erosion of the samples the sputtering time was reduced to 5 min.

## Non-sputtered samples

The samples **4**–**6** contain various amounts of products of surface corrosion (Fe oxide phase) and contamination (cf. Table 4 above, Fig. 8b, blue lines). The surface Fe oxidic phase is hydroxylated (cf. broadening of O 1 s spectra in the region of high $E_b$, which is typical for the presence of –OH

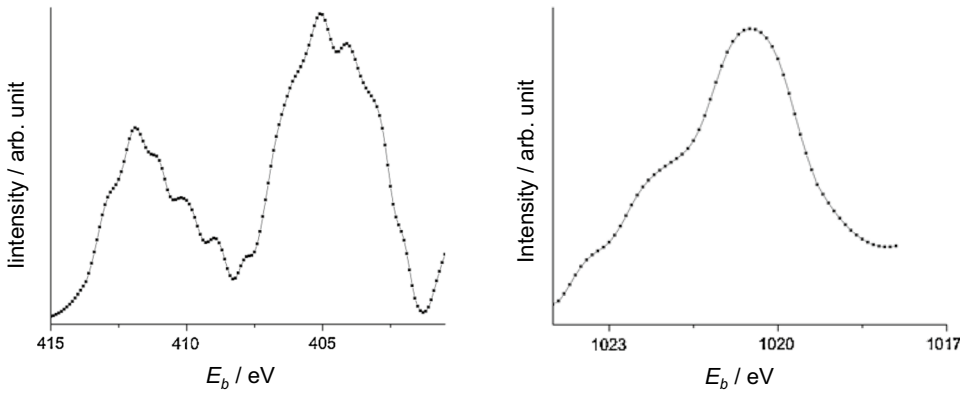


**Fig. 7** The photoelectron spectrum of Cd $3d_{5/2,3/2}$ observed in the sample **6** and Zn $2p_{3/2}$ observed in the sample **7**

**Table 4** Surface concentrations of Fe, C, O, Cd, Pb, and Zn in the samples **1**–**7** expressed as at.%

| Sample | Si | Fe | C | O | Cd | Pb | Zn |
|---|---|---|---|---|---|---|---|
| **1** $Fe^0$ powder, bare | 5.7 | 18.2 (60.5)[a] | 38.3 (31.3) | 37.8 (8.2) | 0 (0) | 0 (0) | 0 (0) |
| **2** $Fe^0$ aged 3 h | 0 | 16.5 (34.3) | 30.4 (32.5) | 53.0 (33.2) | 0 (0) | 0 (0) | 0 (0) |
| **3** $Fe^0$ aged 10 days | 0 | 21.7 (36.3) | 37.4 (31.1) | 41.0 (32.6) | 0 (0) | 0 (0) | 0 (0) |
| **4** $Fe^0$ aged 3 h + $Zn^{2+}$ | 0 | 17.3 (29.4) | 45.7 (43.0) | 36.7 (27.6) | 0 (0) | 0 (0) | 0.3 (0.0) |
| **5** $Fe^0$ aged 3 h + $Pb^{2+}$ | 0 | 10.1 (20.8) | 42.0 (28.1) | 36.8 (49.6) | 0 (0) | 2.1 (1.5) | 0 (0) |
| **6** $Fe^0$ aged 3 h + $Cd^{2+}$ | 0 | 10.1 (18.4) | 42.0 (34.6) | 45.8 (46.5) | 0.5 (0.5) | 0 (0) | 0 (0) |
| **7** $Fe^0$ aged 3 h + $Zn^{2+}$ + $Pb^{2+}$ + $Cd^{2+}$ | 0 | (23.8) | (23.0) | (51.4) | (0) | (1.2) | (0.5) |

[a]Numbers in brackets belong to the XPS measurements after $Ar^+$ ion sputtering

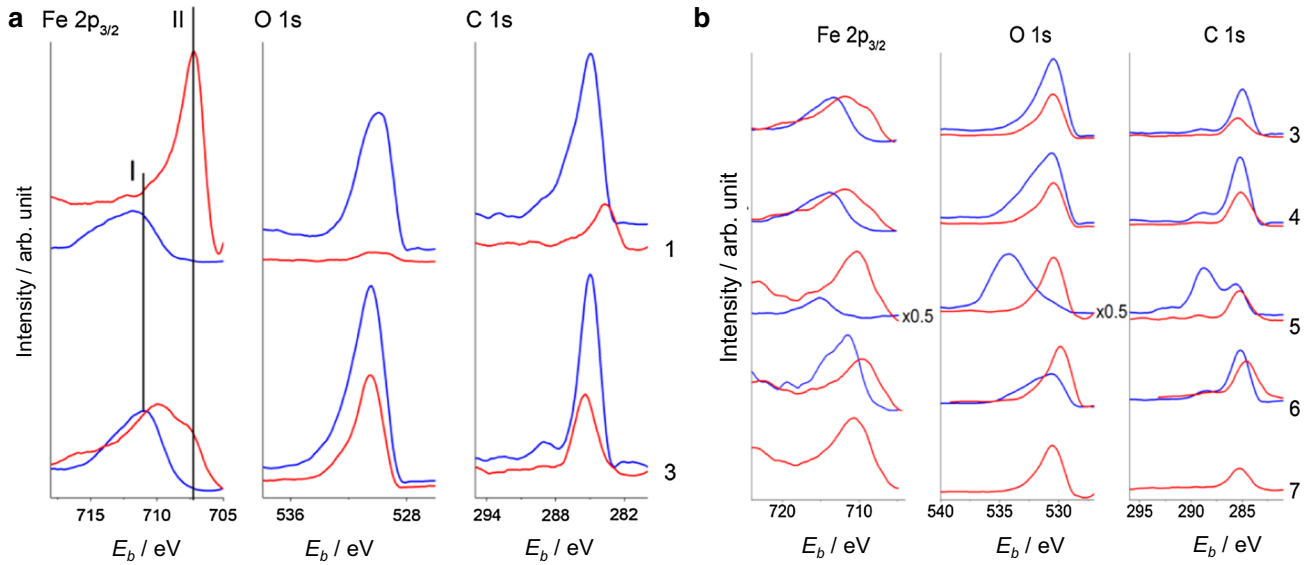


**Fig. 8** **a** Comparison of the Fe $2p_{3/2}$ O 1 s and C 1 s spectra of the samples **1** and **3**. Blue color: before $Ar^+$ sputtering, red color: after $Ar^+$ sputtering. **b** The Fe $2p_{3/2}$, O 1 s and C 1 s photoelectron spectra before (blue) and after (red) $Ar^+$ sputtering for 7 min (sample **3**) and 5 min (samples **4**–**7**). Intensities of the photoelectron spectra are normalized relative to the intensity of Fe 3p spectrum

groups). This Fe oxide phase could be ascribed to FeOOH resulting from surface hydroxylation and subsequent dehydration of the exposed iron in aqueous solution as reported Xi et al. [42].

The line shapes of the photoelectron spectra of the sample **5** are deformed by differential charging. This sample is covered by the phase which is in poor electrical contact with its surface, which induces differential charging, which disables discussion of the line shapes of photoelectron spectra in this case. On non-sputtered samples, Zn (sample **4**), Pb (sample **5**), and Cd (sample **6**) have been observed (Fig. 9a). Hydrocarbon contamination present on the surfaces is composed mostly from aliphatic hydrocabons (C 1 s line at ~ 285 eV, Fig. 8b).

## Sputtered samples

Rather similar effect of sputtering is observed for the samples **4**–**7**. Much thicker oxide layer remained on the sample surfaces after their short (5 min) time sputtering (cf. absence of low energy shoulder in the Fe $2p_{3/2}$ spectrum of the samples **4**–**7** (Fig. 8b). However, the high energy asymmetry of the O 1 s spectra is reduced, i.e. only small concentration of hydroxylated Fe oxide phase remained after sputtering (Fig. 8b). Hydrocarbon contamination is also reduced (C 1 s spectra in Fig. 8b). No differential charging is observed in the sputtered sample **5**.

In agreement with the Table 4, where data for all elements (except Fe) are mostly lower after sputtering, we can conclude that a substantial part of the precipitated phase on the surfaces (together with the adsorbates) of the samples **4**–**7** was eliminated by sputtering. Thus, Pb is adsorbed on the samples **5**, **7**, Cd is adsorbed on the sample **6**, and Zn on the sample **7** (pertinent spectra cf. Fig. 9a). However, the extent of erosion of the oxidic coating of Fe grains by sputtering is not clear.

The Pb $4f_{7/2,5/2}$ photoelectron spectra observed in the samples **5** and **7** are depicted in Fig. 9b. The spectrum was simulated by two doublets (sample **5**) and three doublets (sample **7**). The doublet I is assigned to $Pb^0$, doublet II to PbO. This result is consistent with those of Xi et al. [42], where their XPS analysis has confirmed that immobilized Pb was present in its zero and bivalent forms. Moreover, the authors proposed that using nano-zero-valent iron, partial reduction of $Pb^{2+}$ takes place following by its precipitation as PbO.

The XPS study points to the contribution of adsorption in the mechanism of removal of heavy metals using aged $Fe^0$. Furthermore, since it was found lead in the oxidation number 0 ($Pb^0$) we can conclude that partial reduction of $Pb^{2+}$ by remaining $Fe^0$ contributes in the removal of $Pb^{2+}$. This mechanism is in straight line with the mechanism reported by Li and Zhang [43], Xi et al. [42]. Moreover, precipitation of lead as $Pb(OH)_2$ (or PbO after drying) also takes place as earlier reported [42].

In the case of $Zn^{2+}$ and $Cd^{2+}$, based on the results of characterization, we can suggest that the removal of both cations depends on the affinity of the respective cation towards FeCPs (adsorption onto FeCPs) which could be according to the present study $Fe_2O_3$ and FeOOH. Nevertheless, co-precipitation should be the other important reaction pathway, as

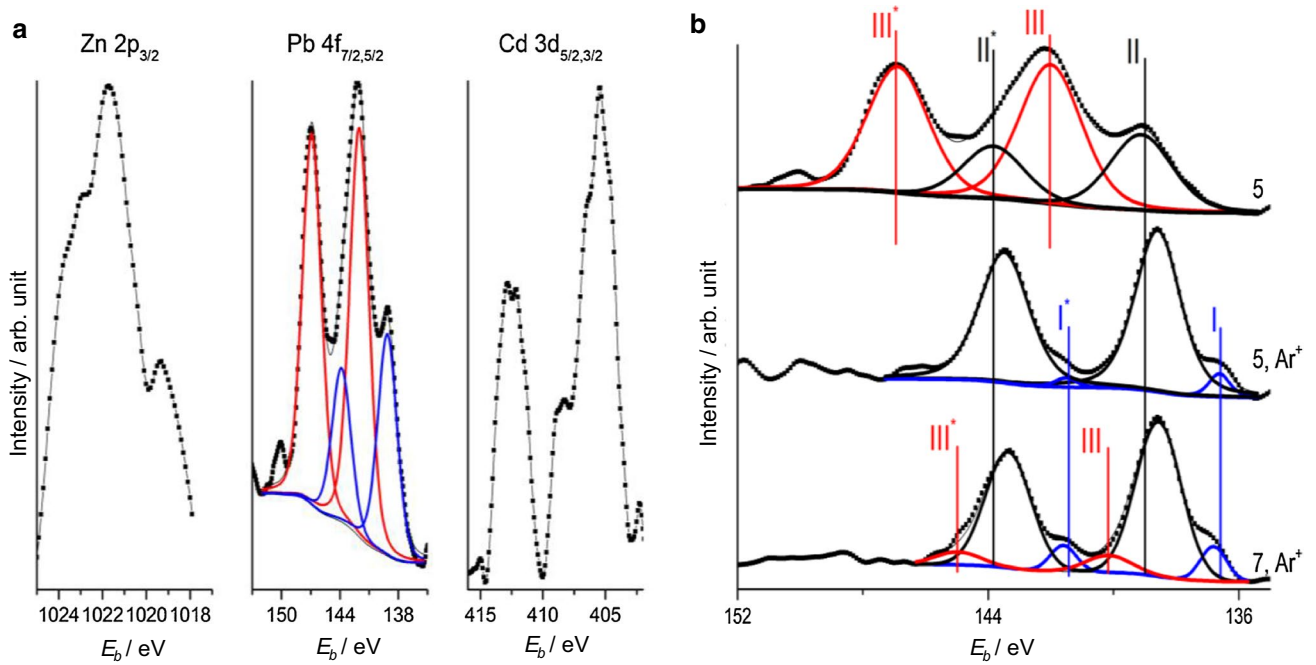


**Fig. 9** **a** Photoelectron spectra of non-sputtered sample **4** (Zn $2p_{3/2}$), **5** (Pb $4f_{7/2,5/2}$), and **6** (Cd $3d_{5/2,3/2}$). (red doublet in Pb 4f spectrum: lines shifted by differential charging); **b** measured and simulated Pb $4f_{7/2,5/2}$ spectra of the sample **5** before $Ar^+$ sputtering (top), and samples **5**, **7** after $Ar^+$ ion sputtering. Blue doublet I, $I^*$: $Pb^0$, black doublet II, $II^*$: PbO, red doublet III, $III^*$: spectrum of PbO affected by differential charging

earlier mentioned Statham et al. [13], Noubactep [23, 44]. It is crucial to point out that the whole discussion has ignored reductive processes but has most rationally discussed the process of $Cd^{2+}$, $Pb^{2+}$ and $Zn^{2+}$ removal in $Fe^0/H_2O$ systems. Thus, reductive transformation, when they occur are mediated by iron corrosion products, mainly $Fe^{2+}$ and $H_2$ species [6, 27, 30].

## Conclusions

This study assessed the efficiency of aged $Fe^0$ powder for the removal of $Zn^{2+}$, $Cd^{2+}$, and $Pb^{2+}$ in binary and ternary systems by monitoring their removal from aqueous solution under various experimental conditions. Results demonstrated the existence of an "induction period" after immersion of $Fe^0$ powder in buffered solutions. The duration of this lag time depends on the used $Fe^0$ amount. The lag time corresponds to the time necessary for generation of sufficient amount of solid iron corrosion products (FeCPs) for cations removal by adsorption and co-precipitation. SEM results confirmed the formation of high specific surface FeCPs.

The attention was aimed to the mutual interference of multiple cations simultaneously present in the sample during their remediation. Rapid removal of $Pb^{2+}$ was observed every time at the initial stage of reaction. In the binary system $Pb^{2+}/Zn^{2+}$ the $Pb^{2+}$ ion delays substantially removal of $Zn^{2+}$ whereas $Zn^{2+}$ ion does not influence the removal of $Pb^{2+}$. In the system $Cd^{2+}/Zn^{2+}$ the presence of $Cd^{2+}$ promotes the removal of $Zn^{2+}$ in solution while the $Zn^{2+}$ ions slightly diminish the percentage of the $Cd^{2+}$ removal. In case of $Cd^{2+}/Pb^{2+}$ mixture, any addition of $Pb^{2+}$ in solution decreases the percentage of removal of $Cd^{2+}$ but the presence of $Cd^{2+}$ does not have any influence on the removal of $Pb^{2+}$. In the ternary system the accelerating effect of $Cd^{2+}$ upon the removal of $Zn^{2+}$ is competitively inhibited by the presence of $Pb^{2+}$.

The following order of decreasing efficiency of removal of metal cations by aged $Fe^0$ was found: $Pb^{2+} > Zn^{2+} > Cd^{2+}$. This order positively correlates with the hardness index of investigated cations which are respectively for $Pb^{2+}$, $Zn^{2+}$, and $Cd^{2+}$ 0.131, 0.115, and 0.081 and also with the values of logarithm of their first hydrolysis constants, −7.6, −9, and −10.1, respectively.

XPS analysis has proven the existence of $Fe_2O_3$ and FeOOH phases as iron corrosion products. Furthermore, XPS analysis of sputtered and non-sputtered samples reveals that the investigated heavy metals were adsorbed onto FeCPs. In the case of multiple cations present simultaneously in the tested solution, they may strongly compete for the same adsorption sites. Their mutual interference, however, reflects not only different adsorptivity, but also different reaction mechanisms of remediation of $Pb^{2+}$, $Zn^{2+}$, and $Cd^{2+}$ which involves (co)precipitation depending on pH

and redox processes where also the dissolved oxygen plays a role.

## Experimental

### Chemicals

The used chemicals: cadmium acetate dihydrate ($Cd(CH_3COO)_2•2H_2O$) and lead acetate trihydrate ($Pb(CH_3COO)_2•3H_2O$) were supplied by Aldrich, whilst zinc acetate dihydrate ($Zn(CH_3COO)_2•2H_2O$), acetic acid sodium salt trihydrate ($CH_3COONa•3H_2O$), and glacial acetic acid ($CH_3COOH$) were of analytical grade. Concentration of acetate buffer pH 5.5 was 0.1 mol/dm$^3$. Ethanol and acetone of analytical grade were furnished by Lachner Company. Various stock solutions of heavy metals in single ($Zn^{2+}$, $Cd^{2+}$, $Pb^{2+}$), binary ($Zn^{2+}/Pb^{2+}$ and $Zn^{2+}/Cd^{2+}$), and ternary ($Zn^{2+}/Cd^{2+}/Pb^{2+}$) systems were prepared by dissolving the appropriate amount of weighed individual metallic salts in 0.1 mol/dm$^3$ acetate buffer pH 5.5. In the single system, the concentration of stock solution was 0.06 mol/dm$^3$ whereas in the stock solutions of binary as well as in ternary systems the concentration of $Zn^{2+}$ remains unchanged (0.06 mol/dm$^3$) only the concentrations of $Cd^{2+}$ and $Pb^{2+}$ vary from 0.03 to 0.12 mol/dm$^3$. The working solution of $Zn^{2+}$ ion was 0.3 mmol/dm$^3$ whereas the concentration of $Cd^{2+}$ and $Pb^{2+}$ were varying from 0.15 to 0.6 mmol/dm$^3$ depending on the investigated ratios.

### Materials

The $Fe^0$ powder utilized in the present study (99.8% $Fe^0$, − 200 mesh, 74 µm, Alfa Aesar) with a specific surface area equal to 13.4 m$^2$ g$^{-1}$, was identical to that used in our previous study and was employed without any further pretreatment [19]. Standard filter papers of 55 mm supplied by Fisher scientific and a vacuum pump of 7. 0 mbar were used to dry selected samples for XPS and SEM analysis.

### Experimental procedure

All experiments regarding the pre-corrosion and corrosion of iron powder as well as heavy metals ions removal were carried out in duplicates at room temperature in open flasks of 500 cm$^3$ in presence of air oxygen (oxic conditions).

### Pre-corrosion

The procedure of pre-corrosion of $Fe^0$ powder as well as that of concentration determination of the $Fe^{2+}$ ion during the pre-corrosion time was similar to that realized in our previous study [19]. Indeed, 0.8 g of $Fe^0$ powder was pre-equilibrated in 199 cm$^3$ of 0.1 mol/dm$^3$ acetate buffer at pH 5.5 for 0–3 days to generate in-situ FeCPs. Throughout the pre-equilibrated period, the flasks with solution containing $Fe^0$ were gently shaken using a bath shaker with periodic linear motion by 10 cm (speed 10 cm s$^{-1}$). For concentration determination of $Fe^{2+}$, amount of 20 cm$^3$ was regularly taken away from the flask at various time intervals and directly subjected to DPP where the concentration of $Fe^{2+}$ was determined from the cathodic peak at − 1.4 V versus saturated calomel electrode (SCE). After this procedure, the analyzed samples (after separation from mercury by decantation) were always put back to the original flask to keep on the aging.

### Effect of competitive cations on the removal of $Zn^{2+}$

Here, the impacts of $Cd^{2+}$ and $Pb^{2+}$ ions on the removal of $Zn^{2+}$ were investigated in binary and ternary systems. Two binary systems were tested ($Zn^{2+}/Pb^{2+}$ and $Zn^{2+}/Cd^{2+}$), where the influence of $Pb^{2+}$ and $Cd^{2+}$, respectively, on the $Zn^{2+}$ removal was studied. In the ternary system, $Zn^{2+}/Cd^{2+}/Pb^{2+}$, the cumulative effect of $Cd^{2+}$ and $Pb^{2+}$ on the removal of $Zn^{2+}$ was investigated. The time dependences of all effects were followed and evaluated.

The batch experiments for the removal of heavy metal ions were carried out by adding of 1 cm$^3$ of stock solutions of heavy metal ions of various concentration (from 0.03 to 0.12 mol/dm$^3$) to the flasks with 199 cm$^3$ of buffer containing 0.8 g of $Fe^0$ (aged for 3 h). All experiments were then monitored during 14 days. Regularly, at various time intervals, 20 cm$^3$ of the mixture ($Fe^0$-heavy metals ions) was carefully withdrawn and rapidly subjected to DPP analysis without any dilution. The $Zn^{2+}$, $Cd^{2+}$, and $Pb^{2+}$ ions were always identified by DPP at − 1.04, − 0.6, and − 0.43 V vs. SCE, respectively. After analysis the solution was put back to the original flask to keep on the aging.

The percentage of metallic cation removal was calculated by means of equation below where $C_o(M^{2+})$ and $C_t(M^{2+})$ are the initial concentration of metallic cation ($M^{2+}$) and that at time $t$, respectively:

$$\%\ \text{of removal of } M^{2+} = \left[\frac{C_o(M^{2+}) - C_t(M^{2+})}{C_o(M^{2+})}\right] \times 100. \quad (1)$$

### Drying of samples for characterization

Seven samples of the iron powder were selected for characterization: six of them, after 14 days reaction time in the presence of air oxygen with differently aged $Fe^0$ were dried before analysis. As a standard (the seventh sample) fresh $Fe^0$ powder was taken directly from the flask without any treatment. Those samples were denoted and described as follows: (**1**) $Fe^0$ powder; (**2**) 0.8 g of $Fe^0$ aged 3 h in 199 cm$^3$

of 0.1 mol/dm$^3$ acetate buffer pH 5.5; (**3**) 0.8 g of Fe$^0$ aged 10 days in 199 cm$^3$ of 0.1 mol/dm$^3$ acetate buffer pH 5.5; (**4**) 0.8 g of Fe$^0$ aged 3 h in 199 cm$^3$ of 0.1 mol/dm$^3$ acetate buffer pH 5.5 plus 1 cm$^3$ of stock solution of $Zn^{2+}$ (0.06 mol/dm$^3$), final concentration of $Zn^{2+}$ 0.3 mmol/dm$^3$; (5) 0.8 g of Fe$^0$ aged 3 h in 199 cm$^3$ of 0.1 mol/dm$^3$acetate buffer pH 5.5 plus 1 cm$^3$ of stock solution of $Pb^{2+}$ (0.06 mol/dm$^3$), final concentration of $Pb^{2+}$ 0.3 mmol/dm$^3$; (**6**) 0.8 g of Fe$^0$ aged 3 h in 199 cm$^3$ of 0.1 mol/dm$^3$ acetate buffer pH 5.5 plus 1 cm$^3$ of stock solution of $Cd^{2+}$ (0.06 mol/dm$^3$), final concentration of $Cd^{2+}$ 0.3 mmol/dm$^3$; (**7**) 0.8 g of Fe$^0$ aged 3 h in 199 cm$^3$ of 0.1 mol/dm$^3$ acetate buffer pH 5.5 plus 1 cm$^3$ of stock solution of $Zn^{2+}$:$Cd^{2+}$:$Pb^{2+}$ (0.06 mol/dm$^3$), ratio 1:1:1, final concentration of each heavy metal equals to 0.3 mmol/dm$^3$.

Those six samples were filtered under vacuum with standard filter paper size 55 mm, and then washed respectively with ethanol and acetone. The obtained dried powders were carefully withdrawn from the paper and kept in a clear container, ready for XPS and SEM analysis.

## Analytical methods

The HI 3220 pH/ORP meter was used for pH determination of the solution.

Differential Pulse Polarography (DPP) was employed for concentration determination of $Fe^{2+}$ and $Zn^{2+}$, $Cd^{2+}$, and $Pb^{2+}$ ions in solution. Differential pulse polarographic curves were recorded with the 663 VA Stand series 05 connected to a digital computer controlled potentiostat PGSTAT 30 (Autolab-Metrohm). Three electrode system was used with mercury drop working electrode, SCE as reference and Pt wire as auxiliary electrode. DPP parameters: scan rate 10 mV/s, modulation peak amplitude 25 mV, modulation time 50 ms, and drop time 1 s [19].

An Omicron Nanotechnology ESCAProbe P spectrometer (Omicron Nanotechnology GmbH, Taunusstein, DE) was used to measure the photoelectron spectra. XPS analysis was performed at a pressure of ~ $10^{-8}$ Pa. The X-ray source was monochromatic at 1486.6 eV. The photoelectron spectra were measured at low resolution (survey spectra in the energy region of 0–1200 eV with a step size of 0.6 eV) and at high resolution in 30 eV scans with a step size of 0.1 eV). The samples were measured before and after sputtering by argon ions ($Ar^+$). The abundance $A(x)$ of the elements in the samples was evaluated in the atomic percents calculated from corrected integral intensities ***I*** of the Fe 3p, C 1s, O 1s, Pb 4f, Zn 2p, and Cd 4d spectra:

$$A(x)\left[\frac{I(x)^{\mathrm{corr}}}{I(\mathrm{Fe\ 3p})^{\mathrm{corr}}+I(\mathrm{C\ 1s})^{\mathrm{corr}}+I(\mathrm{O\ 1s})^{\mathrm{corr}}+I(\mathrm{Pb\ 4f})^{\mathrm{corr}}+I(\mathrm{Cd\ 4d})^{\mathrm{corr}}+I(\mathrm{Zn\ 2p})^{\mathrm{corr}}}\right]\times 100. \quad (2)$$

It can be assumed the presence of the precipitated phase created by dissolution of the powder on the grains surface. To test this possibility the photoelectron spectra were measured as received samples and after their soft argon ion $Ar^+$ sputtering ($E = 5$ keV, $i \sim 5$ mA, $t = 5$ min, 7 min). Possible surface precipitated phase might be reduced by this treatment. Sputtering can erode the samples surface, however. Damped nonlinear least-squares fitting procedure was used to distinguish partially resolved lines in the Pb 4f photoelectron spectra measured in high resolution [45]. Minimal number was used in simulation of the spectra. Assignment of the photoelectron lines was done by comparison of estimated binding energies B.E. (eV) with standard ones [46]. The samples were dried before XPS experiment. The effect of aging of Fe powder in buffered water ambient is investigated first. Then the samples exposed to buffered water ambient which contained $Zn^{2+}$, $Cd^{2+}$, and $Pb^{2+}$ ions are characterized. Metal ions can be present on the Fe powder during aging period (i.e. due to adsorption from water ambient) or during drying of the samples (i.e. as a contamination). We tried to resolve the both of this mechanism by XPS analysis of the samples as received and after cleaning by argon ($Ar^+$) ion sputtering.

For SEM analysis, the S 4800-I scanning electron microscope (Hitachi, Tokyo, Japan) was utilized and acceleration voltage of 5 kV was applied.

**Acknowledgements** The authors are grateful namely to the institutional support of the J. Heyrovský Institute of Physical Chemistry, Czech Academy of Sciences, RVO 61388955.

## References

1. Gosar M (2004) Geoenviron 51:2097
2. Xiao R, Wang S, Li R, Wang JJ, Zhang Z (2017) Ecotox Environ Safe 141:17
3. Oldright GL, Keyes HE, Miller V, Sloan WA (1928) Precipitation of lead and copper from solution on sponge iron. Bulletin 281, Bureau of Mines, p 131
4. Bojic AL, Bojic D, Andjelkovic T (2009) J Hazard Mater 168:813
5. Vollprecht D, Plessl K, Neuhold S, Kittinger F, Öfner W, Müller P, Mischitz R, Sedlazeck KP (2020) Processes 8:279

6. Xiao M, Hu R, Cui X, Gwenzi W, Noubactep C (2020) Processes 8:409
7. O'Hannesin SF, Gillham RW (1998) Ground Water 36:164
8. Henderson AD, Demond AH (2011) Environ Eng 137:689
9. Kishimoto N, Iwano S, Narazaki Y (2011) Water Air Soil Pollut 221:183
10. Guan X, Sun Y, Qin H, Li J, Lo IMC, He D, Dong H (2015) Water Res 75:224
11. Noubactep C (2015) Water Res 85:114
12. Suponik T, Winiarski A, Szade J (2015) Water Air Soil Pollut 226:360
13. Statham TM, Mumford KA, Stark SC, Gore DB, Stevens GW (2015) Sep Sci Technol 50:2427
14. Vollprecht D, Krois LM, Sedlazeck KP, Müller P, Mischitz R, Olbrich T, Pomberger R (2018) J Clean Prod 208:1409
15. Devonshire E (1890) J Frankl Inst 129:449
16. Lauderdale RA, Emmons AH (1951) J Am Water Works Ass 43:327
17. Gatcha-Bandjun N, Noubactep C, Loura Mbenguela B (2014) Fresenius Environ Bull 23:2663
18. Gatcha-Bandjun N, Noubactep C, Loura Mbenguela B (2017) Environ Technol Innov 8:71
19. Touomo-Wouafo M, Donkeng-Dazie J, Btatkeu-K BD, Tchatchueng JB, Noubactep C, Ludvík J (2018) Chemosphere 209:617
20. Nde-Tchoupé AI, Nanseu-Njiki CP, Hu R, Nassi A, Noubactep C, Licha T (2019) Chemosphere 219:855
21. Phukan M, Noubactep C, Licha T (2015) Chem Eng J 259:481
22. Hildebrant B, Ndé-Tchoupé AI, Lufingo M, Licha T, Noubactep C (2020) Processes 8:265
23. Noubactep C (2007) Open Environ Sci 1:9
24. Noubactep C (2008) Environ Technol 29:909
25. Ghauch A (2015) Freiberg Online Geosci 32:1
26. Gheju M (2018) Water 10:651
27. Hu R, Yang H, Tao R, Cui X, Xiao M, Konadu-Amoah B, Cao V, Lufingo M, Soppa-Sangue NP, Ndé-Tchoupé AI, Gatcha-Bandjun N, Sipowo-Tala VR, Gwenzi W, Noubactep C (2020) Water 12:641
28. Cantrell KJ, Kaplan DI, Wietsma TW (1995) J Hazard Mater 42:201
29. Qiu SR, Lai HF, Roberson MJ, Hunt ML, Amrhein C, Giancarlo LC, Flynn GW, Yarmoff JA (2000) Langmuir 16:2230
30. Scott TB, Popescu IC, Crane RA, Noubactep C (2011) J Hazard Mater 186:280
31. Khorshidi N, Azadmehr AR (2017) Desalin Water Treat 58:106
32. Christophi CA, Axe L (2000) J Environ Eng 126:66
33. Forbes EA, Posner AM, Quirk JP (1976) J Soil Sci 27:154
34. Gadde RR, Laitmen HA (1974) Anal Chem 46:2022
35. Lavine BK, Auslander G, Ritter J (2001) Microchem J 70:69
36. Kinraide TB, Yermiyahu U (2007) J Inorg Biochem 101:1201
37. Nesic S (2007) Corros Sci 49:4308
38. Lazzari L (2008) General aspects of corrosion. Encyclopedia of hydrocarbons, chapter 9.1, vol V. Istituto Enciclopedia Italiana, Rome
39. Boparai HK, Joseph M, O'Carroll DM (2013) Environ Sci Pollut Res 20:6210
40. Pawluk K, Fronczyk J (2015) Pol J Chem Technol 15:7
41. Wagner CD, Davis LE, Zeller MV, Taylor JA, Raymond RH, Gale LH (1981) Surf Interface Anal 3:211
42. Xi Y, Mallavarapu M, Naidu R (2010) Mater Res Bull 45:1361
43. Li XQ, Zhang WX (2007) J Phys Chem C 111:6939
44. Noubactep C, Btatkeu-K BD, Tchatchueng JB (2011) Chem Eng J 178:78
45. Kwok RWM (1999) XPSPeak, Version 4.1. Hong Kong, Available online: https://www.phy.cuhk.edu.hk/surface/XPSPeak. Accessed on 21 Sept 2019
46. Briggs D, Seah MP (1996) Practical surface analysis by Auger and X-ray photoelectron spectroscopy. Wiley, New York
47. Schultz MF, Benjamin MM, Ferguson JF (1987) Environ Sci Technol 121:863
48. Benjamin MM (1981) J Coll Inter Sci 79:209
49. Kinniburgh DG, Jackson ML, Syer JK (1976) Soil Sci Soc Am J 40:796